



Effect of Thickness on the Electrical and Optical Properties of Sb Doped SnO₂ (ATO) Thin Films

T.R. GIRALDI,^{*,1} M.T. ESCOTE,¹ M.I.B. BERNARDI,¹ V. BOUQUET,³ E.R. LEITE,¹ E. LONGO¹ & J.A. VARELA²

¹CMDMC/LIEC/DQ UFSCar, Av. Washington Luiz, km 235, São Carlos-SP-Brazil

²CMDMC/LIEC/IQ, Unesp, R. Prof. Francisco Degni, s/n, Araraquara-SP-Brazil

³LCSIM, Institut de Chimie de Rennes, Université de Rennes 1, Rennes Cedex 35 042, France

Submitted March 5, 2003; Revised May 14, 2004; Accepted July 30, 2004

Abstract. This work reports the preparation and characterization of (SnO₂) thin films doped with 7 mol% Sb₂O₃. The films were prepared by the polymeric precursor method, and deposited by spin-coating, all of them were deposited on amorphous silica substrate. Then, we have studied the thickness effect on the microstructural, optical and electric properties of these samples. The microstructural characterization was carried out by X-ray diffraction (XRD) and scanning tunneling microscopy (STM). The electrical resistivity measurements were obtained by the van der Pauw four-probe method. UV-visible spectroscopy and ellipsometry were carried out for the optical characterization. The films present nanometric grains in the order of 13 nm, and low roughness. The electrical resistivity decreased with the increase of the film thickness and the smallest measured value was $6.5 \times 10^{-3} \Omega \text{ cm}$ for the 988 nm thick film. The samples displayed a high transmittance value of 80% in the visible region. The obtained results show that the polymeric precursor method is effective for the TCOs manufacturing.

Keywords: thin film, tin oxide, antimony

Introduction

Transparent conductive oxides (TCO) have been extensively studied, due to their important potential technological applications, such as in flat-panel displays, solar cells or other optoelectronic devices, among others [1]. For these applications, it is desired a combination of good transparency in the visible spectral range with low resistivity. Tin oxide is one of the few pure semiconductors that presents good transmittance in the visible region. It is the simplest oxide of non-cubic structure that also presents stable *d* orbitals [2]. The stoichiometry, along with the nature, quantity and microstructural distribution of dopants play an important role on the electrical properties of SnO₂ [3].

Several studies show that SnO₂ in presence of the dopant Sb⁵⁺ (ATO) displays low resistivity, remaining

transparent in wavelength that includes the visible region. Therefore, this system has been extensively studied in the last years [4–8]. Electrical resistivity in the order of $10^{-3} \Omega \text{ cm}$ and transparency close to 80% have been observed in these works. Such properties allow SnO₂-based materials to be applied in electrooptical systems. A variety of methods have been used to deposit antimony doped tin oxide thin films. These include sputtering [4], spray-pyrolysis [5], electron-beam [6], sol-gel [7], and dip-coating of polymeric precursor solution [8].

In this work, thin films of SnO₂:Sb were obtained by spin-coating of a polymeric precursor solution. This method presents some advantages relative to other methods, such as low cost and the excellent quality (good homogeneity and low roughness) of the films. The resulting surface condition is suitable for the TCO application, and permits the production of films with high transmittance and low resistivity. As far as we know, few works report a systematic studies concerning

*To whom all correspondence should be addressed. E-mail: tania@liec.ufscar.br

the electrical, optical and structural characterization of SnO₂:Sb thin films prepared by polymeric precursors [8]. In this sense, this paper reports on an investigation of the thickness effect on the structural, electrical and optical properties of antimony-doped tin oxide SnO₂:Sb thin films.

Experimental Procedure

The polymeric precursor method consists in the polymerization of a metallic citrate with ethylene glycol. Hence, to prepare the tin oxide films, it was necessary to obtain a tin citrate. The raw materials for this synthesis were: tin chloride, citric acid and ammonium hydroxide. The molar proportion among these reactants was 1:3:1, respectively. Tin chloride was dissolved to an aqueous acid citric solution, along with ammonium hydroxide (for the pH control), resulting in the precipitation of tin citrate. In this case, the pH must be carefully controlled and must not exceed 3, in order to avoid the co-precipitation of tin hydroxide. In addition, to the elimination of Cl⁻ ions, the precipitate was washed with distillate water until the filtered water displays no trace of Cl⁻ ions. For this, we have added silver nitrate (AgNO₃) to this water and verify if occur the formation of AgCl precipitate.

Then, 7 mol% Sb₂O₃ and citric acid was added to this tin citrate that was stirring and heated until the formation of a polymeric resin. Nitric acid was added to dissolve the components. Afterwards, ethylene glycol was added to promote the polyesterification reaction. The solution was heated to 90°C to eliminate NO_x gases and to accelerate the polymerization.

The resulting transparent resin was clear and presented a yellowish color. The viscosity of the resin was adjusted to 30 mPas by controlling the water content. The thin films were deposited onto amorphous silica substrates. The precursor solution was deposited by the spin-coating technique. The rotation velocity and time were fixed at 3800 rpm and 30 s, respectively. After deposition, the substrates were dried on a hot plate (~150°C), followed by a two-stage heat treatment. In the first stage, the films were heated to 300°C, with a heating rate of 1°C/min, for 2 h, promoting the pyrolysis of the organic material. In the second stage, the films were heated to 650°C with a 5°C/min rate and soaking time of 2 h, followed by cooling down at the same rate. Similar heat treatment conditions are used in a previous work [8].

The crystalline structure of the films was studied by means of X-ray diffraction (XRD). It was performed on a Siemens D5000 diffractometer, equipped with LiF (100) monochromator and using Cu K α radiation at a grazing incident angle. The microstructure was observed by scanning tunneling microscopy (Digital Instruments-Nanoscope III-A). The optical transmittance measurements were made in an UV-Vis-NIR (Cary 5G spectrophotometer), and the refraction index and thickness were observed by ellipsometry (Jobin Yuon). The electrical resistivity and Hall effect of the films was measured by using the van der Prawn method (PPMS 6000 Quantum Design).

Results and Discussion

In order to study the crystallinity and structural characteristics of the SnO₂:Sb (7 mol%) thin films, we have characterized them by X-ray Diffraction XRD. The diffractograms of these films with different thickness are shown in Fig. 1. This figure revealed X-ray patterns that show Bragg reflections belonging to the SnO₂:Sb polycrystalline phase. The (*hkl*) indexes (not shown) were assigned on the basis of the tetragonal rutile phase of SnO₂, and the lattice parameters were evaluated for all films. Through this data, we observed *a* and *c* values close to ~4.740(2) Å and ~3.188(2) Å, respectively, and these values seem to be independent of the film thickness. Also, these values are in good agreement with those reported in literature for the Sb-doped SnO₂ (6.2%) and they are slight higher than the lattice parameters found for the undoped SnO₂ [9]. These results could be associated to the different size of the Sb⁵⁺ and Sn⁴⁺. From these results, we verified that there is no trace of additional phases and we can assume that antimony formed at least a partial solid solution with SnO₂. However, it is possible the occurrence of a relaxation phenomena, in which the heat treatment drive the Sb dopant from the inner lattice sites towards the surface of the grain. It results in a non-homogeneous solid solution in the grains, such behavior have already been reported in the literature for Mn, La, Ce, and Y-doped SnO₂ [10, 11]. If it occurs, we believe that it could promote change in the transport of these SnO₂:Sb films. In fact, according to the literature [12], the presence of other phases similar the system results in higher electrical resistivity values, due to a decrease of the electronic mobility and an increase on the quantity of interfaces between the Sb₂O₃ and SnO₂ phases.

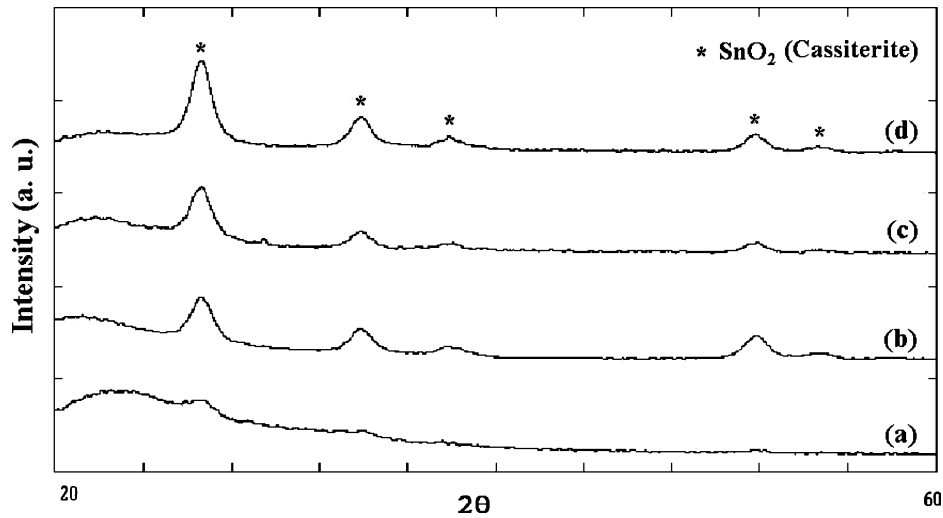


Fig. 1. X-ray diffractograms of the $\text{SnO}_2:\text{Sb}$ thin films with a: (a) 150 nm, (b) 388 nm, (c) 600 nm, and (d) 988 nm thickness.

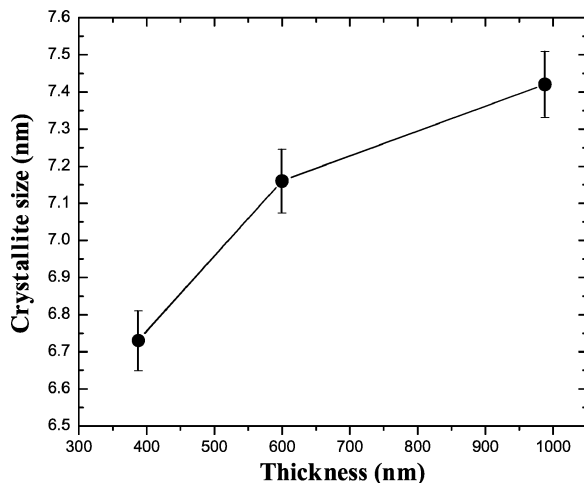


Fig. 2. Crystallite size as a function of the film thickness.

The observed effect of the thickness on the diffractogram characteristics changes solely the peak intensities and not the peak positions. This can be explained by an increase on the crystallite size with increasing film thickness. Figure 2 illustrates the crystallite size as a function of the film thickness. The crystallite size was estimated from the X-ray patterns using the Scherrer equation [13]. The increase of the crystallite with increasing thickness can be associated to longer heat treatments to which the thicker films were submitted.

Morphological information of these thin film surfaces was analyzed by the STM technique, such as grain

sizes and shapes and the surface roughness. Figure 3 illustrates bidimensional and tridimensional STM images of a 988 nm thick film. Through this figure, we observed that the films present a spherical-type grains with nanometric average grain size close to ~ 13 nm. The average grain size is rather higher than that estimated from the crystallographic data (see Fig. 2). We believed that it could be related to a possible agglomeration of crystallites in these films. Although, the formation of a nanometric grains is related to the Sb^{5+} substitution on the $\text{SnO}_2:\text{Sb}$ thin films, several works reported that the dopant in SnO_2 should increase the stresses in this matrix and therefore reduce the grain growth [14, 15]. Such behavior, in general, was associated to an enrichment of Sb on the surface of the grains, which could result in non-homogeneous solid solution of the $\text{SnO}_2:\text{Sb}$ samples [15]. In addition, the thin film surface roughness R_q values are relatively low, with values ranging from the $R_q \sim 0.40$ to 0.65 nm. Such R_q values were comparable and even lower than those varying from 1.3 to 39 nm reported in the literature [5, 16–18]. It should be noticed that the processing technique has a great effect on the surface roughness.

At this point, it is important to observe the importance of the morphology on the physical properties of the $\text{SnO}_2:\text{Sb}$ thin films. In the case, several studies reported on the contribution of grain boundaries on the electrical properties in non-nanometric semiconductor [10]. For such compounds, it is assumed that the lack of homogeneity in the grain boundary could promote

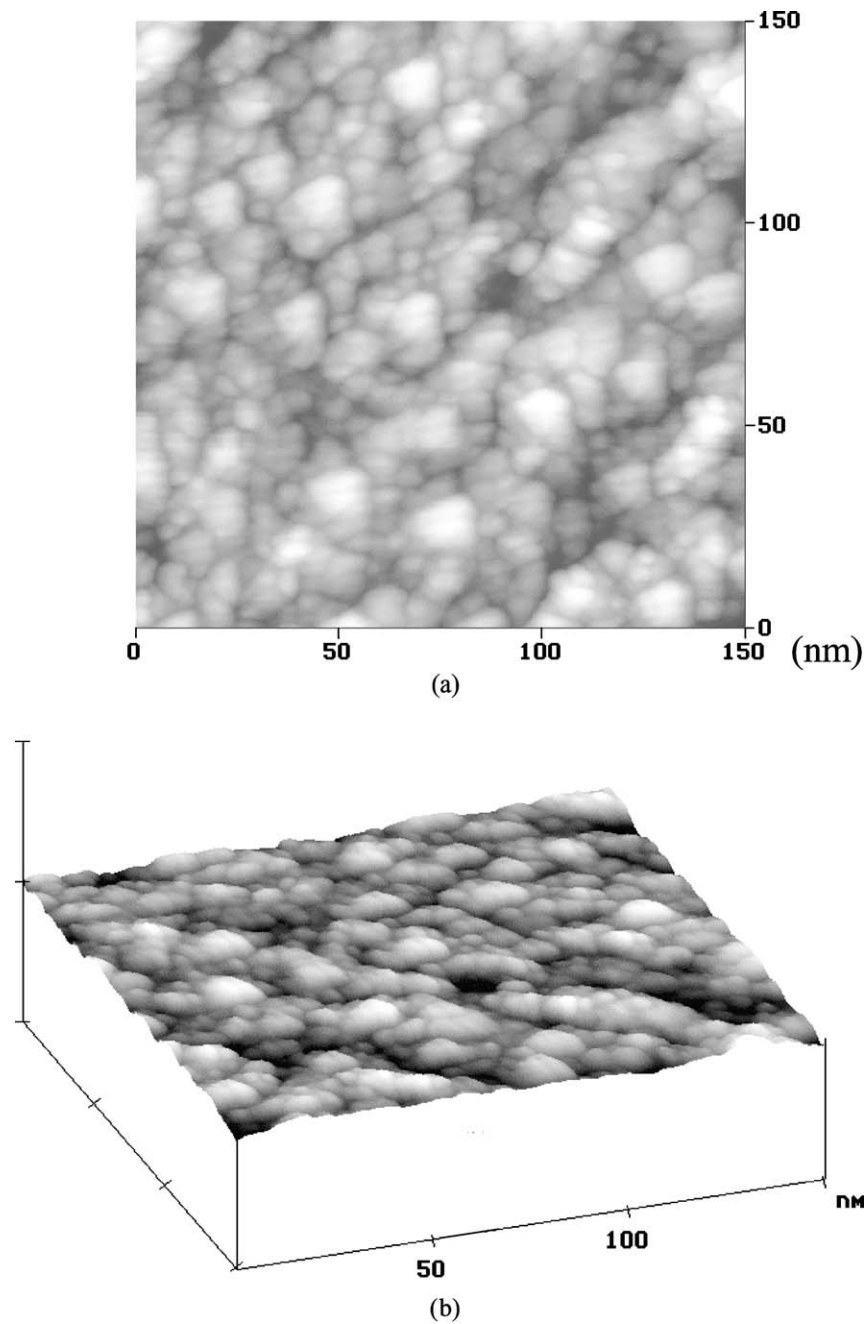


Fig. 3. STM images of the 988 nm-thick SnO₂:Sb film.

the formation of a potential barrier across the depletion region, which inhibits the transport of electrons among grains, also called charge-trapping model [19]. Otherwise, the work developed by Leite et al. [20] showed that nanometric grains display a higher electrical con-

ductivity σ with low contribution of the grain boundary. In this case, the high σ is related to the homogeneous distribution of the carriers through the grain, differently from the non-nano-sized grain in which the σ is associated to trapped carriers in the grain boundary. In

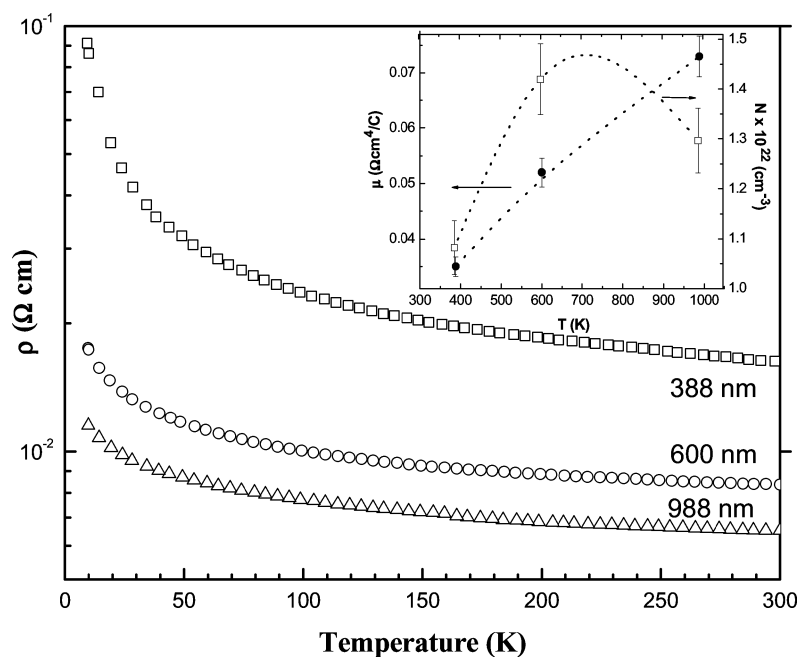


Fig. 4. Temperature dependence of the electrical resistivity as a function of the temperature for thin films of SnO₂:Sb with different thickness. The inset shows the hall mobility (μ) and the number of carriers (N) measured for the SnO₂:Sb thin films. The dashed line is just a guide to view.

addition, Bruneaux [21] showed that for similar nano-sized compounds, with higher charge carrier number, the grain boundary effect has low contribution to the total conductivity and the main contribution for the electrical conductivity is due the electron mobility inside the grain. Therefore, we believe that the main contribution for the electrical conductivity of the SnO₂:Sb thin films is also due to the electron mobility inside the grain.

Figure 4 displays the electrical resistivity $\rho(T)$ as a function of temperatures performed on the SnO₂:Sb films. The lowest measured $\rho(T)$ value at room temperature was $6.5 \times 10^{-3} \Omega \text{ cm}$ in a 988 nm thick film. This result is in good agreement with the existing results found in the literature, reporting on this type of films obtained by more other techniques, include sputtering [4], spray-pyrolysis [5], and electron-beam [6]. Analyzing these data at room temperature, it can also be observed that there is a clear decrease of $\rho(T)$ values with increasing film thickness. This change of the electrical resistivity values may be attributed mainly to three different contribution due to: (a) microstructural defects, (b) increase of the crystallinity degree, and (c) the scattering of charge carrier by the film surface. In or-

der to verify this point, Hall effect measurements were performed to these films. These data revealed one small increase of the Hall mobility μ and number of carriers N when the thickness of the sample is increased from 388 to 600 nm. However, the samples with thickness 600 to 988 nm seem to have almost the same N values. In this sense, we believed that such difference in the $\rho(T)$ values of the films with different thickness could be associated mainly with the changes in the mobility of the electrons. These results are in good agreement with those obtained by Gasparro et al. [22]. Then, the decrease of the film resistivity with thickness observed in this work is related to the increase of carrier mobility, which could occur due to the decrease of the effect of the scattering of the charge carrier by the film surface. In fact, similar behavior was reported in literature for several kinds of thin films [23].

Figure 5 illustrates a transmittance-wavelength spectrum obtained by optical spectroscopy. It can be observed in the visible light range that for the 600 nm- and 988 nm-thick films the red absorption is more intense than the blue absorption. In the infrared range the absorption is intense, what is expected, since the free electrons are able to absorb in the IR. The band gap

Table 1. Optical constants evaluated of the SnO₂:Sb thin films.

Thickness (nm)	Refraction index	Transmittance (%) 632 nm
150	1.40	90
388	1.40	89
600	1.45	82
988	1.45	77

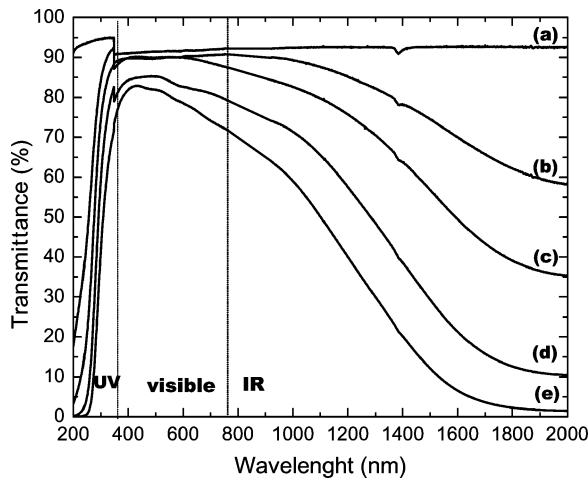


Fig. 5. Transmittance spectra of Sb-doped SnO₂ films deposited onto amorphous silica substrates with different thickness: (a) substrate, (b) 150 nm, (c) 388 nm, (d) 600 nm, and (e) 988 nm.

energies of the films were calculated from the optical spectra using the Wood method [24]. Regardless of the number of layers, the band gap energy values of the thin films were kept at approximately 4.6 eV. It is interesting to notice that the shift of the plasma frequency with the thickness observed in this figure suggested that the thicker films display higher mobility and slightly higher number of carrier. It is in good agreement with the Hall effect measurements, as is shown in the inset of Fig. 4.

Table 1 presents the optical constants of the SnO₂:Sb thin films. From these data, it can be observed that all the films presented high transmittance values and that the refraction index is practically independent of the thickness. This indicates that an increase on the thickness does not promote changes of antimony distribution in the SnO₂ lattice.

Conclusions

High quality polycrystalline SnO₂:Sb thin films were deposited on the amorphous silica substrate by spin

coating of a polymeric precursor solution. The films showed high electrical conductivity and high transmittance in the visible light range. The electrical resistivity values clearly decrease as the thickness of the films increases, and we have obtained ρ (300 K) values as low as $6.5 \times 10^{-3} \Omega \cdot \text{cm}$ for a 988 nm thick film. This decrease of the electrical resistivity with film thickness could be attributed to the lesser relative contribution of the carrier scattering at the film surface. Thin films presented transparency in the order of 80% in the visible spectrum and refractive index remained almost constant with the change of the film thickness.

With this work, it is concluded that the polymeric precursor method provide a production of high quality and homogeneous polycrystalline SnO₂:Sb thin films. It is very important for a possible technological application of these films as electro-optical devices.

Acknowledgments

Authors would like to thank to CAPES, CNPq and FAPESP by the financial support of this research project.

References

1. R.G. Gordon, *MRS Bull.*, **25**, 52 (2000).
2. Z.M. Jarzebski and J.P. Marton, *J. Electrochem. Soc.*, **123**, 199 (1976).
3. K.C. Mishra, K.H. Johnson, and P.C. Schmidt, *Phys. Rev. B*, **51**, 13972 (1995).
4. S. Jäger, B. Szyszka, J. Szyczyrbowski, and G. Bräuer, *Surf. Coat. Tech.*, **98**, 1304 (1998).
5. S. Shanthi, C. Subramanian, and P. Ramasamy, *Journal of Cryst. Growth*, **197**, 858 (1999).
6. E.K.H. Shokr, *Semicond. Sci. Tech.*, **15**, 247 (2000).
7. C. Terrier, J.P. Chatelon, and J. A. Roger, *Thin Solid Films*, **295**, 95 (1997).
8. M.I.B. Bernardi, L.E. Soledade, I.A. Santos, E.R. Leite, E. Longo, and J.A. Varela, *Thin Solid Films*, **405**, 228 (2002).
9. B. Grzeta, E. Tkalec, C. Goebbert, M. Takeda, M. Takahashi, K. Nomura, and M. Jaksic, *J. Phys. Chem. Solids*, **63**, 765 (2002).
10. D. Gouvêa, A. Smith, J.P. Bonnet, and J.A. Varela, *J. Eur. Ceram. Soc.*, **18**, 345 (1998).
11. E.R. Leite, A.P. Maciel, I.T. Weber, P.N. Lisboa-Filho, E. Longo, C.O. Paiva-Santos, A.V.C. Andrade, C.A. Paskocimas, Y. Maniette, and W.H. Schreiner, *Adv. Mater.*, **14**, 905 (2002).
12. K.H. Kim and S.W. Lee, *J. Am. Ceram. Soc.*, **77**, 915 (1994).
13. B.D. Cullity, *Elements of X-Ray Diffraction* (Addison Wesley Publishing Company, Massachusetts, 1967), p. 170.

14. C. Terrier, J.P. Chatelon, J.A. Roger, R. Berjoan, and C. Dubois, *J. Sol-gel Sci. Techn.*, **10**, 75 (1997).
15. E.R. Leite, I.T. Weber, and E. Longo, *Adv. Mat.*, **12**, 965 (2000).
16. S. Jäger, B. Szyszka, J. Szczyrbowski, and G. Bräuer, *Surf. Coat. Tech.*, **98**, 1304 (1998).
17. C. Savaniu, A. Arnautu, and C. Cobianu, *Thin Solid Films*, **349**, 29 (1999).
18. J. Szanyi, *Appl. Surf. Sci.*, **185**, 161 (2002).
19. T.I. Kamins, *J. Appl. Phys.*, **42**, 4357 (1971).
20. E.R. Leite, M.I.B. Bernardi, E. Longo, J.A. Varela, and C.A. Paskocimas, *Thin Solid Films*, **449**, 67 (2004).
21. J. Bruneaux, H. Cachet, M. Froment, and A. Messad, *Thin Solid Films*, **197**, 129 (1991).
22. G. Gasparro, J. Putz, D. Ganz, and M.A. Aegerter, *Sol. Energ. Mat. Sol. C.*, **54**, 287 (1998).
23. M. Ohring, *The Materials Science of Thin Films* (Academic Press, Inc., 1992), p. 457.
24. D.L. Wood and J. Tauc, *Phys. Rev. B*, **5**, 3144 (1971).